

Nonstationary coherence effects in pulsed excitation of hyperfine structure transitions in optically oriented atoms

N. A. Dovator and R. A. Zhitnikov

A. F. Ioffe Physicotechnical Institute, Academy of Sciences of the USSR, Leningrad

(Submitted 30 December 1978)

Zh. Eksp. Teor. Fiz. 77, 505-518 (August 1979)

Nonstationary radio frequency (RF) coherence signals from optically oriented atoms are observed and investigated during the excitation of hyperfine-structure transitions by microwave magnetic-field pulses, unmodulated, or modulated to the Zeeman-splitting frequency. Radio frequency coherence nutation and free-precession signals are experimentally recorded. Multiple spin RF coherence echo signals excited by two successive microwave pulses are detected. A RF coherence echo signal is also detected after the passage of a single microwave pulse and the subsequent inversion of the magnetic-field gradient. The observed effects are analyzed theoretically in the approximation of a three-level quantum system impulsively perturbable by two variable resonance magnetic fields. Agreement between the experimental results and the theory is obtained.

PACS numbers: 32.30.Bv, 32.90.+a, 32.70.Jz

O.S. Vasyutinskii and the present authors have observed and investigated¹ radiofrequency (RF) coherence of atomic states corresponding to the Zeeman sublevels of optically oriented atoms during the excitation of hyperfine structure (HFS) transitions by a microwave magnetic field modulated in amplitude at the Zeeman-splitting frequency. The investigations were carried out on cesium atoms. The radiofrequency coherence arose as a result of the simultaneous excitation of two HFS transitions having a common level. Similar effects were subsequently observed during the optical pumping of potassium vapor.² In the investigations published in Refs. 3 and 4, RF coherence was recorded for the case of a two-quantum excitation of HFS transitions (with the use of microwave and RF quanta).

In the previous investigations¹⁻⁴ stationary RF coherence signals were investigated. Also of interest is the investigation of the behavior of RF coherence during the simultaneous pulsed excitation of two abutting HFS transitions. What is more, since the RF coherence in this case is due to the appearance of a transverse component of the magnetization, the appearance of nonstationary coherence effects—nutation, free precession, and spin echo—is, by analogy with normal magnetic resonance,⁵ to be expected here. The present paper is devoted to the observation and theoretical investigation of such nonstationary RF-coherence signals from optically oriented atoms.

Transient coherence processes in three-level systems have been observed also in optical spectroscopy⁶⁻⁸ and NMR.^{9,10} In the present investigation we were able to detect a number of previously unobserved coherence effects, as, for example, multiple spin echo and complex nutation of the RF coherence.

1. EXPERIMENTAL PROCEDURE

A block diagram of the experimental setup is shown in Fig. 1. The experiment was performed with ¹³³Cs atoms. Pumping light from the cesium lamp 1, in which an electrodeless HF discharge was excited, after passing through the interference filter 2, which transmitted

only the D_1 cesium line ($\lambda = 8943 \text{ \AA}$), and the circular polarizer 3, entered the absorption cell 4, which was filled with cesium vapor and a buffer Ne or Ar gas (the signals shown in this paper correspond to a cell containing Ne at a pressure of 80 Torr). The change occurring in the absorption of the pumping light by the cell at the time of magnetic resonance was recorded by the photodetector 5, the signal from which was amplified by the broadband amplifier 6 and recorded by the oscillograph 7. The constant magnetic field H_0 was produced by the Helmholtz coils 8. The source of the microwave magnetic field, which induced the HFS transitions in the cesium atoms, was the 3-cm-band microwave generator 9, which had a maximum output power of 500 mW. The rectangular horn-type antenna 10 was oriented with respect to the H_0 field in such a way that both the $\pi(\Delta m_F = \pm 1)$ and $\sigma(\Delta m_F = 0)$ magnetic-dipole HFS transitions could be excited. The switching on and switching off of the microwave power flux entering the cell 4 were effected with the aid of the SHF diode 11, which was controlled either with the aid of radio pulses from the radiofrequency generator 12, or by video pulses from the pulse generator 13. The first case corresponded to pulsed switching on of the microwave field, whose amplitude was modulated at a frequency equal to the frequency of the generator 12 and with a modulation index of 100%.

The coherence between the Zeeman sublevels $F = 4$,

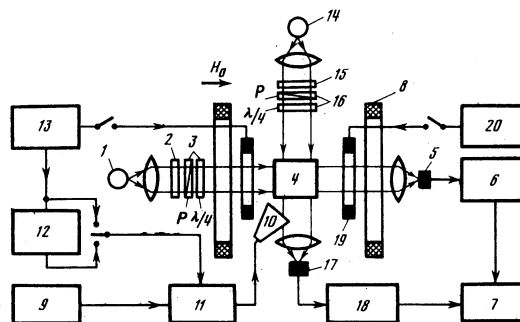


FIG. 1. Block diagram of the experimental setup.

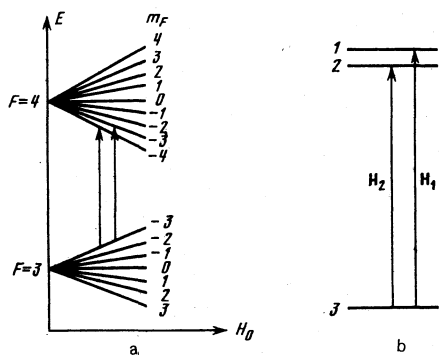


FIG. 2. a) Energy level scheme for the ground state of the cesium atom in a weak magnetic field. b) Diagram of a three-level quantum-mechanical system. The arrows indicate the ^{133}Cs HFS transitions excitable in experiment.

$m_F = -4$ and $F = 4, m_F = -3$ (Fig. 2a) of the ^{133}Cs atoms, which was investigated in the experiment, was recorded from the absorption of a transverse—to H_0 —light beam from the cesium lamp 14 after it had passed through the interference filter 15, which transmitted only the D_1 line of ^{133}Cs , and the circular polarizer 16. The detection of the absorption of the transverse light beam was carried out by the photodetector 17, the signal from which was fed to the oscillograph 7 via the amplifier 18. For the experiments on the observation of RF coherence echo signals, we produced an artificial nonuniformity in the magnetic field with the aid of the opposing coils 19, which were powered by the constant-current source 20, and which, for the purpose of reversing the magnetic-field gradient, was fed with a video pulse from the generator 13.

2. EXPERIMENTAL RESULTS

We first of all generated and investigated a RF coherence free-precession signal (under "RF-coherence free-precession" we mean the behavior of the RF coherence after the microwave radiation has been switched off). To generate it, we used an amplitude-modulated microwave magnetic-field pulse whose carrier frequency was adjusted beforehand to the resonance HFS-transition frequency, while the modulation frequency coincided with the Zeeman splitting frequency of the interfering levels.

Figure 3a shows a free-precession signal of the RF coherence between the $F = 4, m_F = -4$ and $F = 4, m_F = -3$ Zeeman sublevels, as recorded from the change in the absorption of the transverse light beam after the expiration of the microwave-field pulse (the microwave-pulse duration $\tau = 200\mu\text{sec}$) tuned to the $(F = 4, m_F = -4) \leftrightarrow (F = 3, m_F = -3)$ HFS-transition frequency, and modulated in amplitude with the frequency $f_0 = 170\text{ kHz}$ [in a field $H_0 = 0.486\text{ Oe}$, $f_0(\Delta F = 0, \Delta m_F = \pm 1) = 170\text{ kHz}$ for ^{133}Cs].

Besides the free-precession signal, we investigated the RF-coherence nutation, by which is meant the modulation of the RF-coherence signal during the action of the microwave pulse. Figure 4b shows a RF-coherence nutation signal generated during the action of a resonance microwave-field pulse of the same characteris-

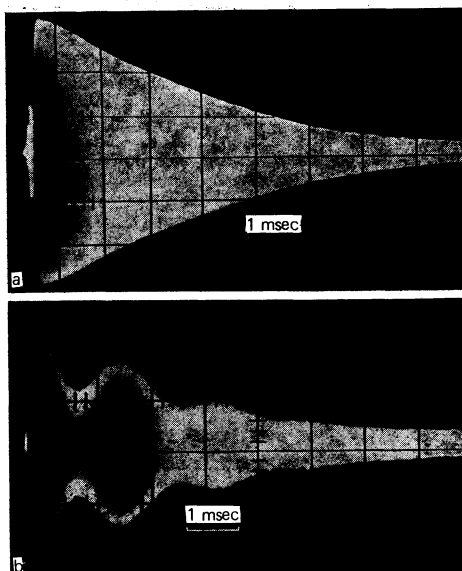


FIG. 3. a) RF-coherence free-precession signal obtained with the aid of an amplitude-modulated microwave radiation pulse tuned on the $(F = 4, m_F = -4) \leftrightarrow (F = 3, m_F = -3)$ HFS transition frequency. b) RF-coherence free-precession signal obtained with the aid of an unmodulated microwave-radiation pulse tuned on the $(F = 4, m_F = -3) \leftrightarrow (F = 3, m_F = -3)$ HFS transition frequency.

tics as the one used in the preceding case, except for the pulse duration, which in this case had the value $\tau = 400\mu\text{sec}$. As can be seen from Fig. 4, the RF-coherence nutation signal has a characteristic shape. What is more, as has been established experimentally, the peak of this signal corresponds to a microwave-pulse duration $\tau = \pi/\Omega_2$, where $2\Omega_2$ is the frequency of the nutation observed in the absorption of a longitudinal light beam^{11a} during the impulsive excitation of the $(F = 4, m_F = -4) \leftrightarrow (F = 3, m_F = -3)$ HFS transition by the fundamental harmonic of a modulated microwave field (in this case

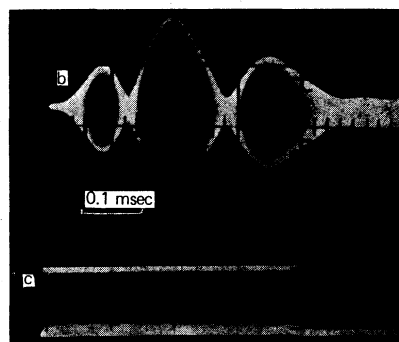
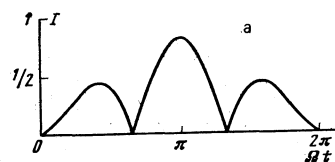


FIG. 4. a) Theoretical signal (in relative units), b) experimental RF-coherence nutation signal, c) microwave-power pulse (frequency of occupation is 170 kHz).

the frequency of the amplitude modulation of the microwave field was adjusted away from the Zeeman splitting frequency).

We also succeeded in obtaining experimentally a RF-coherence spin echo signal under the conditions of a nonuniform magnetic field. The nonuniformity of the the magnetic field in the volume of the cell was produced with the aid of the coils 19 in Fig. 1. The RF-coherence echo signals were generated by two methods. In the first of them, which is similar to the Hahn method,¹² we used a train of two microwave pulses. In this case we observed in the experiment, besides the echo signal that appeared after the second microwave pulse within an interval of time equal to the interval between the microwave pulses, two additional echo signals characterized by a long time lag. It has been experimentally established that different exciting-microwave-pulse durations correspond to the maximum amplitudes of the various echo signals. Thus, the greatest amplitude of the first echo signal is observed when the microwave-pulse durations are equal, i.e., when $\tau_1 = \tau_2 = \pi/\Omega_2$, whereas shorter microwave pulses are required for the subsidiary echo signals. In Fig. 5a we show an oscillogram of the subsidiary RF-coherence echo signals, obtained for the optimal—for their simultaneous observation—values of $\tau_1 = \tau_2 = 70 \mu\text{sec}$ (the experimentally determined value of the frequency $\Omega_2 = 6\pi \times 10^3 \text{ rad/sec}$).

As the second method of generating the echo signals, we used the method¹³ in which the gradient of the constant magnetic field is reversed after the passage of a single microwave pulse. For this purpose, to the coils 19 in Fig. 1, which were connected to the direct-current source 20, were fed a rectangular current pulse from the generator 13, which led to the magnetic field's being reversed twice.

Figure 6 shows RF-coherence echo signals obtained by reversing the magnetic-field gradient ($G = 2 \times 10^{-3} \text{ Oe/cm}$) at the moments of time marked by the arrows on the figure. In this case the microwave-pulse duration was $\tau = \pi/\Omega_2$, which corresponded to the greatest echo amplitudes.

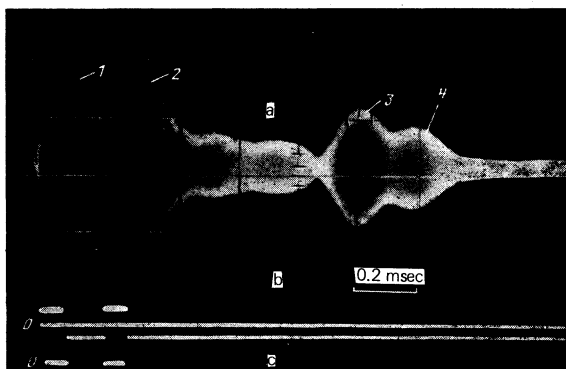


FIG. 5. a) Oscilloscope traces of the subsidiary RF-coherence spin echoes (3, 4). (The signals 1 and 2 are free precession signals, generated after the passage of the SHF pulses.) b) Microwave-radiation pulses. c) Current in the coils 19 in Fig. 1.

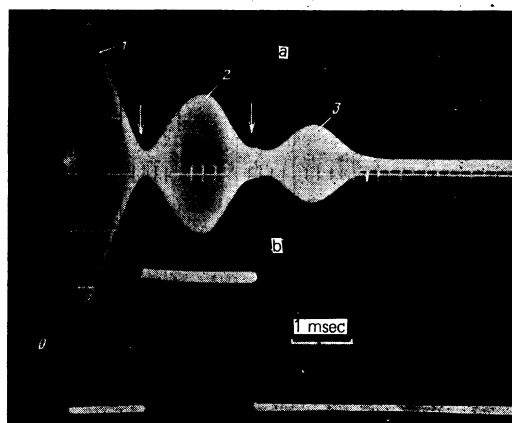


FIG. 6. a) Oscilloscope traces of RF-coherence spin-echo signals (2, 3) (The signal 1 is a free-precession signal, generated after the passage of the microwave pulse.) b) Current in the coils 19 in Fig. 1.

It should be noted that, compared to the echo signals obtained by the magnetic-field-gradient inversion method, the multiple-echo signals excited by two microwave pulses possess a significantly lower intensity. They could be recorded only when the maximum power (500 mW) of the microwave generator 9 (in Fig. 1) was used and the magnetic-field inhomogeneity in the interval between the microwave pulses and after the second microwave pulse was impulsively enhanced (Fig. 5c). This is due to the fact that it is difficult in the case of a stationary magnetic-field gradient to meet the condition for the total excitation of the inhomogeneously broadened HFS-transition lines and, hence, obtain the maximum echo amplitude (the inhomogeneous line widths of the $\Delta F = 1$, $m_F = -4 \leftrightarrow m_F = -3$; $\Delta F = 1$, $m_F = -3 \leftrightarrow m_F = -3$ HFS transitions are respectively equal to $7\gamma\Delta H_0$ and $6\gamma\Delta H_0$, where ΔH_0 is the inhomogeneity of the magnetic field in the cell volume and $\gamma/2\pi = 350 \text{ kHz/Oe}$).

Besides the nonstationary coherence effects observed during the action of pulses of microwave radiation modulated in amplitude with the frequency of the Zeeman splitting of the interfering levels, we succeeded in observing nonstationary RF-coherence signals (free precession, nutation, and spin echo) with the aid of a microwave-field pulse without amplitude modulation, but tuned on the frequency of one of the HFS transitions.

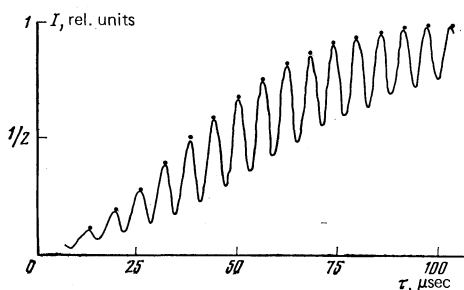


FIG. 7. Dependence of the initial amplitude of the RF-coherence free-precession signal on the duration of the unmodulated microwave-radiation pulse tuned on the ($F = 4$, $m_F = -3$) \leftrightarrow ($F = 3$, $m_F = -3$) transition frequency. The magnetic-field strength $H_0 = 0.486 \text{ Oe}$.

Figure 3b shows a RF-coherence free precession signal, generated after the action of a microwave pulse that was of duration $\tau = 96 \mu\text{sec}$, and tuned on the ($F=4, m_F=-3$) \rightarrow ($F=3, m_F=-3$) HFS transition.

Section 3c of the present paper is devoted to the theoretical explanation of this signal. Therefore, let us note here only a few of its distinctive features. First, as can be seen from Fig. 3b, this signal is amplitude modulated and, secondly, its initial amplitude is a periodic function of the duration of the exciting microwave pulse (Fig. 7).

3. DISCUSSION OF THE EXPERIMENTAL RESULTS

a. *Radiofrequency-coherence spin-echo signals excited with the aid of amplitude-modulated microwave radiation pulses.* In considering this effect in the system composed of the sublevels of the $6^2S_{1/2}$ ground state of ^{133}Cs (Fig. 2a), we shall consider only three levels (Fig. 2b), since an amplitude-modulated microwave magnetic field excites transitions only between three levels. For the sake of simplicity, we shall also neglect the effect of the relaxation and diffusion processes on the echo signals.

Let us find the solution to the Schrödinger equation for a three-level atom that is at one of the levels $i=1, 2, 3$ at the initial moment of time, i.e., at $t=0$:

$$i\hbar \frac{\partial \Psi(\mathbf{r}, t)}{\partial t} = (\hat{\mathcal{H}}_0 + \hat{V}) \Psi(\mathbf{r}, t), \quad (1)$$

where $\Psi(\mathbf{r}, t)$ is the wave function of the atom, $\hat{\mathcal{H}}_0$ is the unperturbed Hamiltonian of the atom, and \hat{V} is the perturbation operator. Following Schenzle *et al.*,¹⁴ we shall seek the solution in stages: the atom is acted upon in the time intervals $0 < t < t_1$ and $t_2 < t < t_3$ (Fig. 8a) by two variable magnetic fields, $\mathbf{H}_2 \cos \omega_2 t$ and $\mathbf{H}_1 \cos \omega_1 t$ (the fundamental and side harmonics of the amplitude-modulated microwave field) that simultaneously excite the two magnetic-dipole transitions $3 \rightarrow 2$ and $3 \rightarrow 1$, respectively, and for which

$$\hat{V} = -\hat{\mu}(\mathbf{H}_1 \cos \omega_1 t + \mathbf{H}_2 \cos \omega_2 t), \quad (2)$$

where $\hat{\mu}$ is the atom's magnetic-dipole-moment operator, while in the time intervals $t_1 < t < t_2$ and $t > t_3$ the atom is in the free state, i.e., $\hat{V} = 0$.

As usual, let us represent $\Psi(\mathbf{r}, t)$ in the form of an expansion in terms of the eigenfunctions of $\hat{\mathcal{H}}_0$:

$$\Psi(\mathbf{r}, t) = \sum_{i=1}^3 C_i(t) \Psi_i(\mathbf{r}) = \sum_{i=1}^3 a_i(t) \exp\left(-i \frac{E_i}{\hbar} t\right) \Psi_i(\mathbf{r}), \quad (3)$$

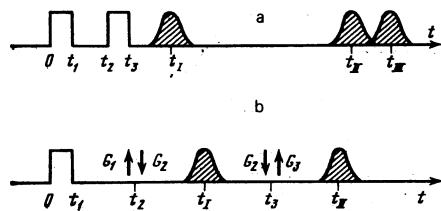


FIG. 8. Scheme for obtaining RF-coherence spin-echo signals: a) with the aid of two microwave pulses, b) with the aid of a microwave pulse and the subsequent inversion of the magnetic-field gradient G .

where $\Psi_i(\mathbf{r})$ and E_i are the eigenfunctions and eigenenergies of the unperturbed Hamiltonian and $a_i(t)$ is the probability amplitude for the state i . Let us note that for the 1, 2, 3 ($F, m_F = 4, -3; 4, -4; 3, -3$) levels of a cesium atom located in a magnetic field $H_0 + \Delta H$, the following relations are fulfilled:

$$E_1 - E_3 \approx \hbar \nu_{\text{HFS}} - 6(E_1 - E_2), \quad E_2 - E_3 \approx \hbar \nu_{\text{HFS}} - 7(E_1 - E_2), \quad (4)$$

$$E_1 - E_2 \approx \hbar \gamma (H_0 + \Delta H),$$

where ν_{HFS} is the hyperfine-splitting frequency for the ^{133}Cs atom, $\gamma/2\pi = 350 \text{ kHz/Oe}$, and H_0 is that magnetic field at the center of the cell which corresponds to the resonance conditions:

$$\omega_1 = (E_1 - E_2)/\hbar = \omega_{12}, \quad \omega_2 = (E_2 - E_3)/\hbar = \omega_{23}. \quad (5)$$

Substituting (3) into (1), we obtain a system of three differential equations for the probability amplitudes $a_i(t)$. Solving this system of equations for $\hat{V} \neq 0$, (2) (the solution is carried out in the resonance approximation: $\omega_1 \approx \omega_{12}$, $\omega_2 \approx \omega_{23}$), as well as for $\hat{V} = 0$, and successively applying the obtained solutions to the corresponding time intervals, we obtain

$$C_i^{(m)}(t > t_3) = \{ \exp[-i(E_i/\hbar)(t_3 - t_2 + t_1) - i\omega_1 t_1 - i(E_i/\hbar)(t - t_3)] \} \times \sum_{j=1}^3 A_{ij}(t_3 - t_2) A_{jm}(t_1) \exp[i(E_j/\hbar)(t_1 - t_2) + i\omega_j(t_2 - t_1)], \quad (6)$$

where $\omega_3 \equiv 0$ and m defines the initial conditions for the atom: $C_i(t=0) = \delta_{im}$, $m = 1, 2, 3$.

The coefficients $A_{ij}(t)$ have the form

$$A_{11} = \sum_{i=1}^3 [p_i(p_i - i\Delta_1) + \Omega_1^2] c_i, \quad A_{22} = \sum_{i=1}^3 [p_i(p_i - i\Delta_1) + \Omega_1^2] c_i,$$

$$A_{23} = \sum_{i=1}^3 (p_i - i\Delta_1)(p_i - i\Delta_2) c_i, \quad A_{12} = A_{21} = (-\Omega_1 \Omega_2) \sum_{i=1}^3 c_i,$$

$$A_{13} = A_{31} = (i\Omega_1) \sum_{i=1}^3 (p_i - i\Delta_2) c_i, \quad A_{32} = A_{23} = (i\Omega_2) \sum_{i=1}^3 (p_i - i\Delta_1) c_i. \quad (7)$$

In (7) we have adopted the notation: $\Delta_k = \omega_k - \omega_{k3}$, $\Omega_k = \frac{1}{2} \mu_{k3} H_k$, μ_{k3} is the component of the matrix element of the dipole moment of the $k \rightarrow 3$ transition in the direction of \mathbf{H}_k , ($k=1, 2$), and

$$c_i^{-1} = \exp(p_i t) \prod_{j=1, j \neq i}^3 (p_i - p_j), \quad \Omega_1^2 + \Omega_2^2 = \Omega^2,$$

where the p_i are the roots of the equation

$$(p - i\Delta_1)\Omega^2 + (p - i\Delta_1)(p - i\Delta_2)p + i(\Delta_1 - \Delta_2)\Omega_1^2 = 0. \quad (8)$$

In the experiment, the registration of the RF coherence was carried out by recording the change in the absorption of a circularly polarized light beam traveling at right angles to \mathbf{H}_0 . As is well known,^{1, 2, 15} in this case the optical-absorption signal, S , will be determined by the element $\rho_{12}(t)$, $\rho_{12} = \rho_{12}^*$, of the density matrix for the ensemble of atoms in the cell. Then, by definition of the density matrix,¹⁶ and taking also into account the fact that the absorption cell is located in a nonuniform magnetic field, we have

$$S \sim \rho_{21}(t > t_3) = \langle \rho_{21}^*(\Delta_2^*, t > t_3) \rangle_{\text{ns}}, \quad (9)$$

where

$$\begin{aligned} \rho_{21}^k(\Delta_2^k, t > t_3) &= \sum_{i=1}^3 C_1^{(i)}(t > t_3) C_2^{(i)}(t > t_3) n_i^0 \\ &= \sum_{i=1}^3 n_i^0 \{ \exp[i(\omega_1 - \omega_2)t_3 + i(E_1^k - E_2^k)(t - t_3)/\hbar] \} \\ &\quad \times \left\{ \sum_{l,m=1}^3 A_{li}^*(t_3 - t_2) A_{li}^*(t_1) A_{2m}(t_3 - t_2) A_{mi}(t_1) \right. \\ &\quad \left. \times \exp[i(E_1^k - E_m^k)(t_3 - t_1)/\hbar + i(\omega_m - \omega_1)(t_3 - t_1)] \right\} \end{aligned} \quad (10)$$

is the element of the density matrix of the k -th of the "isochromatic" atom groups into which the ensemble of atoms in the cell can be divided.¹⁷ An isochromatic group is formed by the atoms located in the same field $H_0 + \Delta H^k$, and having, consequently, the same detunings $\Delta_2^k = 7\gamma\Delta H^k$, $\Delta_1^k = 6\gamma\Delta H^k$, which follows from (4). The coefficients $C_1^{(i)}$, $C_2^{(i)}$ are given by the expression (6), n_i^0 is the relative population of the i -th level of the ground state of cesium, and $\langle \dots \rangle_k$ denotes averaging over all the isochromatic atom groups.

Taking account of the fact that the energy of 1, 2, 3 levels satisfies the relation, (4), we can easily see from (9) and (10) that we should observe at the moments of time

$$t_I = t_3 + (t_2 - t_1), \quad t_{II} = t_3 + 6(t_2 - t_1), \quad t_{III} = t_3 + 7(t_2 - t_1)$$

RF-coherence echo signals determined respectively by the terms in (10) with $l, m = 2, 1; 1, 3; 2, 3$. Indeed, at the moment of time t_I only the phase of the $(l, m = 2, 1)$ term, which has the amplitude

$$|A_{12}(t_3 - t_2)|^2 \sum_{i=1}^3 n_i^0 A_{2i}^*(t_1) A_{1i}(t_1),$$

will be the same for all the isochromatic groups of atoms of the cell, the phases of the remaining terms in (10) being different for different groups.

Thus, the RF coherence will be partially rephased at $t = t_I$, and this partial rephasing is the cause of the appearance of the echo signal. Similar arguments are valid for the moments of time t_{II} and t_{III} . Then the amplitude of the RF-coherence echo at the moments of time t_I, t_{II}, t_{III} will have the form

$$S(t_j) = \left| \int_{\Delta_{2\min}}^{\Delta_{2\max}} [A_{1i}^*(t_3 - t_2) A_{2m}(t_3 - t_2) \sum_{i=1}^3 n_i^0 A_{li}^*(t_1) A_{mi}(t_1)] g(\Delta_2) d\Delta_2 \right|, \quad (11)$$

where $j, l, m = I, 2, 1; II, 1, 3; III, 2, 3$ and $g(\Delta_2)$ is the normalized distribution function of the atoms over the magnetic field in the cell:

$$\int_{\Delta_{2\min}}^{\Delta_{2\max}} g(\Delta_2) d\Delta_2 = 1.$$

In order to compute the integrate (11), we must solve Eq. (8). In the general case the solution of this cubic equations has a fairly complex form.¹⁸ However, the solution can be simplified, since the term

$$i(\Delta_1 - \Delta_2)\Omega_1^2 = -1/8\Delta_1\Omega_1^2$$

in (8) is negligible compared to the term $-i\Delta_1\Omega_1^2$, inasmuch as the experimentally determined quantity $\Omega_2^2/\Omega_1^2 = 9$. Then the solution to Eq. (8) has the form

$$p_1 = i\Delta_1 = 1/8\Delta_2, \quad p_{2,3} = 1/2i(\Delta_2 \pm \alpha); \quad \alpha = (\Delta_2^2 + 4\Omega_2^2)^{1/2}. \quad (12)$$

Using the expressions, (7), for $A_{lj}(t)$ and the solution

(12), and also taking into account the fact that the condition, $|\Delta_2/\Omega| \ll 1$, $\Delta_{2\min} \leq \Delta_2 \leq \Delta_{2\max}$, for the total excitation of the inhomogeneously broadened HFS transition lines, we obtain

$$S(t_I) = \left| \left(\frac{\Omega_1\Omega_2}{\Omega^2} \right)^2 n_2^0 [\cos \Omega(t_3 - t_2) - 1]^2 \left\{ \frac{\Omega_2^2}{\Omega^2} (\cos \Omega t_1 - 1) \right. \right. \\ \left. \left. \times \left[\frac{n_1^0}{n_2^0} + \frac{\Omega_1^2}{\Omega_2^2} + \cos \Omega t_1 \left(1 + \frac{n_1^0 \Omega_1^2}{n_2^0 \Omega_2^2} \right) \right] + \frac{n_3^0}{n_2^0} \sin^2 \Omega t_1 \right\} \right|, \quad (13)$$

$$S(t_{II}) = \left| \frac{\Omega_1\Omega_2^3}{\Omega^4} n_2^0 \left[1 + \frac{\Omega_1^2}{\Omega_2^2} \cos \Omega(t_3 - t_2) \right] \sin \Omega(t_3 - t_2) \right. \\ \left. \times \sin \Omega t_1 \left[\cos \Omega t_1 \sum_{i=1}^3 \frac{n_i^0 \Omega_1^2}{n_2^0 \Omega^2} - \frac{\Omega_2^2}{\Omega^2} \left(1 - \frac{n_1^0}{n_2^0} \right) \right] \right|, \quad (14)$$

$$S(t_{III}) = \left| \frac{\Omega_1\Omega_2^3}{\Omega^4} n_2^0 [\cos \Omega(t_3 - t_2) - 1] \sin \Omega(t_3 - t_2) \right. \\ \left. \times \sin \Omega t_1 \left[\cos \Omega t_1 \sum_{i=1}^3 \frac{n_i^0 \Omega_1^2}{n_2^0 \Omega^2} + \frac{\Omega_1^2}{\Omega^2} \left(1 - \frac{n_1^0}{n_2^0} \right) \right] \right|, \quad (15)$$

where $\Omega_3^2 = -\Omega^2$.

From the expressions (13)–(15) we can easily derive the optimal conditions for the observation of RF-coherence echo signals if we allow for the values of n_1^0 ($n_1^0 = 0.11$, $n_2^0 = 0.233$, $n_3^0 = 0.026$; for their calculation, see Sec. 3b), as well as for the quantity $\Omega_2^2/\Omega_1^2 = 9$. Then, as can be seen from (13), the maximum amplitude of the echo appearing at the moment t_I is attained when the durations of the microwave pulses are equal, i.e., when $t_1 = t_3 - t_2 = \pi/\Omega \approx \pi/\Omega_2$. In their turn, it follows from (14) and (15) that the maximum amplitudes of the echoes for t_{II} and t_{III} are obtained with shorter pulses (for t_{II} , $t_1 \approx 0.7\pi/\Omega$, $t_3 - t_2 \approx \pi/2\Omega$; for t_{III} , $t_1 \approx \pi/4\Omega$, $t_3 - t_2 = 2\pi/3\Omega$).

All the three RF-coherence spin-echo signals that appear respectively at the moments of time t_I , t_{II} , and t_{III} were observed in the experiment. As an example, in Fig. 5a we show the experimentally obtained and theoretically predicted two subsidiary RF-coherence echo signals (in Fig. 5a the echo signal corresponding to the moment t_I is not visible both because of the non-optimal conditions of its excitation ($\tau_1 = \tau_2 = 70 \mu\text{sec}$ for $\Omega_2 = 6\pi \times 10^3 \text{ rad/sec}$) and, especially, because of the free precession that occurs after the second microwave pulse, and prevents its observation). It should also be noted that the theoretically obtained values for the optimal microwave-pulse durations and the conclusion that the RF coherence is partially rephased at the moments t_I , t_{II} , t_{III} explain both the empirical values of the optimal durations of the exciting microwave pulses and the small sizes of the multiple-echo signals, in spite of the measures taken in the experiment to ensure the most exact fulfillment of the condition $|\Delta_{2\max}/\Omega| \ll 1$ (see Sec. 2).

Let us now find the amplitude of the RF-coherence echo obtainable with the aid of an amplitude-modulated microwave field pulse, and following the inversion of the magnetic-field gradient. As in the preceding case, let us divide the solution of the problem into a number of successive stages:

1. When $0 < t < t_1$ (Fig. 8b), two variable fields, $H_1 \cos \omega_1 t$ and $H_2 \cos \omega_2 t$, act on an atom located in the magnetic field $H_0 = \Delta H_1^k$.
2. When $t_1 < t < t_2$ the atom is in the free state in the field $H_0 + H_1^k$.

3. At the moment $t=t_2$ the gradient of the magnetic field is reversed, and the atom finds itself in a magnetic field of strength $H_0 + \Delta H_2^*$.

Solving Eq. (1) in much the same way as the equation for the case of multiple spin echo was solved, we obtain

$$\rho_{21}(t > t_2) = \left\langle \sum_{i=1}^k n_i^0 \left\{ \exp[i(\omega_i - \omega_2)t_1 + i\gamma H_0(t - t_1) + i\gamma \Delta H_1^*(t_2 - t_1) + i\gamma \Delta H_2^*(t - t_2)] A_{i,1}^*(t_1) A_{21}(t_1) \right\} \right\rangle_k. \quad (16)$$

It follows from (16) that, if for any k -th isochromatic group of atoms $\Delta H_1^* = n \Delta H_2^*$ ($n < 0$), then a RF-coherence echo signal should be observed at the moment of time $t = t_2 - n(t_2 - t_1)$. And, in contrast to the preceding two-pulse method, complete rephasing of the RF coherence produced by the microwave pulse occurs in this case.

The amplitude of the RF coherence for the case when the gradient inversion is perfect ($n = -1$) and the condition $|\Delta_{2\max}/\Omega| \ll 1$ is fulfilled has at the moment of time $t = 2t_2 - t_1 \equiv t_1$ the following form

$$S_1 = \left| \frac{\Omega_1 \Omega_2}{\Omega^2} n_2^0 \left\{ \frac{\Omega_1^2}{\Omega^2} (\cos \Omega t_1 - 1) \cdot \left[\frac{n_1^0}{n_2^0} + \frac{\Omega_1^2}{\Omega_2^2} + \cos \Omega t_1 \left(1 + \frac{n_1^0 \Omega_1^2}{n_2^0 \Omega_2^2} \right) \right] + \frac{n_2^0}{n_2^0} \sin^2 \Omega t_1 \right\} \right|, \quad (17)$$

where $\Omega_2^2/\Omega_1^2 = 9$, $n_1^0 = 0.11$, $n_2^0 = 0.233$, $n_3^0 = 0.026$.

As can be seen from (17), the maximum amplitude of the echo is attained when the microwave-pulse duration $t_1 = \pi/\Omega \approx \pi/\Omega_2$. Furthermore, calculations similar to the preceding ones predict the appearance of a second echo signal at the moment $t_{11} = 2(t_2 - t_1) + t_1$ if the gradient is reversed again at $t = t_3 > t_2$ ($\Delta H_2^* = -\Delta H_3^*$) (Fig. 8b).

The echo signals that were obtained in the experiment when the magnetic-field gradient was reversed (Fig. 6) are in accord with the results of the theory.

b. The RF-coherence nutation signal. Let us consider in greater detail the first part of the solution to the problem of the RF coherence spin echo, i.e., of the behavior of $\rho_{12}(t)$ during the action of the microwave pulse ($0 < t < t_1$). Using the solution to Eq. (1) for $V \neq 0$, (2), and also taking into consideration the initial (i.e., $t=0$) distribution of the atoms among the 1, 2, and 3 levels, we find that, for the resonance case, i.e., for $\Delta_1 = \Delta_2 = 0$, the amplitude of the RF-coherence signal is

$$|\rho_{21}(0 < t < t_1)| = S_1 \quad \text{at } t_1 = t. \quad (18)$$

In order to construct the theoretical dependence of $|\rho_{21}(t)|$ on the microwave-pulse duration, we must know the populations of the n_1^0 , n_2^0 , and n_3^0 levels. Since in the experiment we used a cell with the high Ne-buffer-gas pressure of 80 Torr, we can use the theory of optical orientation for the case of total mixing in the excited state^{11b} to estimate the populations of the ($F, m_F = 4, -3; 4, -4; 3, -3$) sublevels of the cesium atom. The values of θ , the optical-relaxation times, and T_1 , the longitudinal-relaxation times, necessary for the computation of the n_i^0 were obtained in an experiment in which the HFS transitions were excited with the aid of the 180-degree pulse method.^{11c} As a result of a calculation with $\theta/T_1 = 0.9$, we obtained for the n_i^0 the values: $n_1^0 = 0.11$, n_2^0

$= 0.233$, $n_3^0 = 0.026$. Figure 4a shows the theoretical curve

$$I = |\rho_{21}(t)| / \frac{\Omega_1 \Omega_2}{\Omega^2} n_2^0,$$

corresponding to these values of n_i^0 and the experimental values $\Omega_2^2/\Omega_1^2 = 9$ and $\Omega_2 = 5\pi \times 10^3$ rad/sec. As can be seen from Fig. 4, there is satisfactory agreement between the experimental and theoretical RF-coherence nutation signals.

c. The nonstationary RF-coherence signals obtained with the aid of an unmodulated microwave-radiation pulse. Besides the nonstationary RF-coherence signals observed with the aid of amplitude-modulated SHF radiation, we also obtained nonstationary signals, using unmodulated microwave-radiation pulses tuned to the frequency of one of the HFS transitions of the cesium atom. As an example, we show in Fig. 3b a RF-coherence free-precession signal obtained with the aid of an unmodulated microwave-radiation pulse tuned to the frequency of the ($4, -3 \rightarrow 3, -3$) transition. The fact that RF-coherence signals are generated under the action of an unmodulated-microwave-field pulse can itself be explained by the broad frequency spectrum of the radiopulse, as a result of which several HFS transitions are excited simultaneously.

As is well known,¹⁹ the modulus of the spectral characteristic of a rectangular radiopulse [$S(t) = A(t) \cos \omega_1 t$; $A(t) = A_1$ when $0 < t \leq \tau$ and $A(t) = 0$ when $\tau < t \leq 0$] has the form

$$|S(\omega)| = (A_1 \tau / 2) \left| \frac{\sin(\omega - \omega_1) \tau / 2}{(\omega - \omega_1) \tau / 2} \right|, \quad (19)$$

where A_1 , ω_1 , and τ are respectively the amplitude, frequency of occupation, and the duration of the radiopulse. It follows from this that the most efficient excitation of the interfering levels characterized by $\Delta F = 0$ and $|\Delta m_F| = 1$ should be realized when the frequency of occupation of the microwave pulse is precisely tuned on the HFS transition, i.e., when $\omega_1 = \omega(\Delta F = 1, \Delta m_F = 0, \pm 1)$, and the pulse duration satisfies the condition

$$\tau = (2n+1)\pi\omega_0^{-1}, \quad (20)$$

where $n = 1, 2, 3, \dots$, and $\omega_0 = \gamma H_0$ is the Zeeman splitting frequency for the interfering levels in the field H_0 .

Figure 7 shows the experimental dependence of the initial amplitude of the free precession of the RF coherence on the duration of a microwave pulse tuned on the ($4, -3 \rightarrow 3, -3$) HFS transition frequency. The points indicate the amplitudes corresponding to the pulse durations computed from the formula (20). As can be seen from the figure, the theory agrees fairly well with the experimental data. A characteristic feature of the signal shown in Fig. 3b is the modulation of the free-precession amplitude. The appearance of this modulation is also due to the broad spectrum of the radiopulse, because of which there occurs a simultaneous excitation of coherence between the ($\Delta F = 0, \Delta m_F = \pm 1$) Zeeman sublevels of both the upper ($F = 4$) and the lower ($F = 3$) hyperfine-structure levels of the cesium atom (Fig. 2a), which differ in the magnitude of the Zeeman splitting. The difference between the Zeeman-splitting frequencies is given by the expression^{11d}

$$\Delta f = (2\pi)^{-1} [\omega_0(F=3) - \omega_0(F=4)] = 2\mu_I H_0 / I \hbar \quad (21)$$

where μ_I is the magnetic moment of the nucleus of the ^{133}Cs atom and I is the nuclear spin. In an $H_0 = 0.486\text{-Oe}$ field, in which the signal shown in Fig. 3b was obtained, $\Delta f = 546\text{ Hz}$, which coincides with the value of the modulation frequency determined experimentally from Fig. 3b.

Thus, we have observed and investigated nonstationary RF coherence (free precession, nutation, spin echo) signals during the impulsive excitation of the HFS transitions of optically oriented cesium atoms. The RF-coherence spin-echo signals were obtained with the aid of either two successive microwave pulses, or one microwave pulse with the subsequent inversion of the magnetic-field gradient. We have obtained for the nonstationary coherence signals theoretical expressions which have allowed us to explain the characteristic SHF-pulse-duration dependence for the nutation signal and the appearance of subsidiary spin-echo signals, as well as to determine the optimal conditions for echo-signal excitation for two methods of realizing it. We have also explained the behavior of the nonstationary signals excited by an unmodulated microwave-radiation pulse. There is good agreement between the experimental results and the theory.

¹O. S. Vasyutinskiĭ, N. A. Dovator, and R. A. Zhitnikov, Zh. Eksp. Teor. Fiz. **72**, 928 (1977) [Sov. Phys. JETP **45**, 484 (1977)].

²E. B. Aleksandrov, A. B. Mamyryn, and Yu. S. Chidson, Zh. Eksp. Teor. Fiz. **72**, 1568 (1977) [Sov. Phys. JETP **45**, 823

(1977)].

³O. S. Vasyutinskiĭ, N. A. Dovator, and R. A. Zhitnikov, Pis'ma Zh. Tech. Fiz. **3**, 360 (1977) [Sov. Tech. Phys. Lett. **3**, 147 (1977)].

⁴O. S. Vasyutinskiĭ, N. A. Dovator, and R. A. Zhitnikov, Pis'ma Zh. Tekh. Fiz. **3**, 462 (1977) [Sov. Tech. Phys. Lett. **3**, 187 (1977)].

⁵A. Abragam, Principles of Nuclear Magnetism, Oxford University Press, Oxford, 1961 (Russ. Transl., IIL, 1963, p. 57).

⁶M. M. T. Loy, Phys. Rev. Lett. **36**, 1454 (1976).

⁷P. Hu, S. Geschwind, and T. M. Jedju, Phys. Rev. Lett. **37**, 1357 (1976).

⁸E. B. Aleksandrov, Avtometriya **3**, 85 (1978).

⁹H. Hatanaka, T. Terao, and T. Hashi, J. Phys. Soc. Jpn. **39**, 835 (1975).

¹⁰H. Hatanaka and T. Hashi, J. Phys. Soc. Jpn. **39**, 1139 (1975).

¹¹N. M. Pomerantsev, V. M. Ryzhkov, and G. V. Skrotskii, Fizicheskie osnovy kvantovoi magnitometrii (The Physical Foundations of Quantum Magnetometry), Nauka, 1972, a) p. 355 b) p. 112, c) p. 358, d) p. 37.

¹²E. Hahn, Phys. Rev. **80**, 580 (1950).

¹³G. J. Béné, Helv. Phys. Acta **45**, 954 (1972).

¹⁴A. Schenzle, S. Grossman, and R. G. Brewer, Phys. Rev. **A13**, 1891 (1976).

¹⁵C. Cohen-Tannoudji, Ann. Phys. (Paris) **7**, 423 (1962).

¹⁶H. E. Puthoff and R. H. Pantell, Fundamentals of Quantum Electronics, Wiley, New York, 1969 (Russ. Transl., Mir, 1972, p. 23).

¹⁷T. P. Das, A. K. Saha, and D. K. Roy, Proc. R. Soc. London Ser. A **227**, 407 (1955).

¹⁸G. Korn and T. Korn, Manual of Mathematics, McGraw Hill, New York, 1967 (Russ. Transl., Nauka, 1970, p. 47).

¹⁹I. S. Gonorovskii, Radiotekhnicheskie tsepi i signaly (Electronic Circuits and Signals), Sov. Radio, 1964, p. 109.

Translated by A. K. Agyei

Relativistic dynamical invariants and the Hamiltonian formalism of charged particles in plane waves

V. Ya. Davydovskii

V. D. Kalmykov Taganrog Radiotechnical Institute

(Submitted 4 April 1979)

Zh. Eksp. Teor. Fiz. **77**, 519-525 (August 1979)

The longitudinal integral of the motion of a charged particle in a plane wave, an integral which is equivalent to conserved particle energy or conserved longitudinal particle momentum in reference systems in which the wave is either stationary or uniform, can be treated as a one-dimensional Hamiltonian if the quantity $kt - \omega z$ is regarded as the time. The validity of the adiabatic invariant that follows from this Hamiltonian is investigated on the basis of the exact equation. Adiabatic invariants that are valid in the particular cases when the above-mentioned adiabatic invariant is not conserved are constructed.

PACS numbers: 03.20. + i

The integrals of, and the adiabatic invariants associated with, the motion of charged particles located in plane periodic electromagnetic fields enable us to investigate such problems as the acceleration of trapped particles when the wave velocity increases and the attendant damping or monochromatization of the waves,¹⁻⁴ the autoresonant motion and radiation of electrons,⁵⁻⁸ stationary nonlinear⁹ and slowly evolving waves in a plasma,¹⁰ semiclassical quantization,¹¹ etc. This incomplete list shows that the dynamical invari-

ants are fairly widely used, and it is therefore useful to generalize this approach, which is the object of the present communication.

Let us consider a plane electromagnetic field that has the nature of a wave, and is described by the potentials

$$A, \varphi = A, \varphi(\psi), \quad \psi = \omega t - kz, \quad (1)$$

where the potentials, the frequency ω , and the wave